Frequency Dependent Lg Q within the Continental United States

Dirk Erickson[1], Daniel E. McNamara[2], and Harley M. Benz[2]

[1] University of Wyoming, Laramie, WY
[2] USGS, Golden, CO

manuscript in preparation: BSSA, October 2003: PREPRINT

Correspondence to:

Dirk Erickson
Department of Geology and Geophysics
P.O. Box 3006
University of Wyoming
Laramie, WY 82071-3006
(307) 766-3363 voice
(307) 766-6679 fax
drericks@uwyo.edu

Abstract

Frequency-dependent crustal attenuation (1/Q) is determined for seven distinct physiographic/tectonic regions of the continental United States using high-quality Lg waveforms recorded on broadband stations in the frequency band 0.5 to 16 Hz. Q(f), is determined for three previously unstudied and four previously studied tectonic regions across the continental United States by inverting Lg frequency-domain amplitudes. Broadband seismic stations record high frequency (0.5 to 16 Hz) energy to determine regional attenuation for Southern and Northern California, the Basin and Range Province, the Pacific Northwest, the Mountain States, Central United States, and the Northeast United States. The Pacific Northwest, Northern California, and the Mountain States regions are new regions where there are no previous Lg Q results. Lg Q is determined at each of the five full octave bands with center frequencies at 0.75, 1.0, 3.0, 6.0, and 12.0 by assuming a geometrical spreading exponent of 0.5 and inverting for Q and source and receiver terms. The frequency-dependent quality factor is often modeled in the form of $Q = Q_o f^{\eta}$. A delete-j Jackknife resampling technique is utilized for error analysis. In general, active tectonic regions have a low Q_o value and a high frequency dependent variable η, whereas stable regions have a high Q_o term and a low value for η. Southern and Northern California, the Basin and Range Province, the Pacific Northwest, and the Mountain States are all tectonically active regions and have frequency-dependent functions of $Q = 152(\pm 37)\, f^{0.72\ (\pm 0.16)}$, $Q = 105(\pm 26)\, f^{0.67\ (\pm 0.16)}$, $Q = 200(\pm 40)\, f^{0.679\ (\pm 0.12)}$, $Q = 152(\pm 49)\, f^{0.761\ (\pm 0.18)}$, and $Q = 166(\pm 37)\, f^{0.61\ (\pm 0.14)}$ respectively. The remaining two regions, Central U.S. and Northeastern U.S., fall into the stable tectonic region category and have frequency-dependent functions of $Q = 640(\pm 225)\, f^{0.344\ (\pm 0.22)}$ and $Q = 650(\pm 143)$

$f^{0.36\ (\pm 0.14)}$. Both scattering and intrinsic attenuation mechanisms are likely to play an equal role for the range of frequencies considered in this study.

INTRODUCTION

Regional attenuation calculations have been derived from the arrival and measurement of Lg wave amplitudes recorded at broadband stations across the continental United States. A large amount of new earthquake data allows us to create a detailed attenuation map of the U.S., which will provide the hazard community with valuable information about shaking intensities at various frequencies for the design of structures including bridges, buildings, and dams. Variations in the attenuation of seismic waves in different tectonic regions was noticed prior to modern day instrumentation when the shaking intensity of earthquakes in the western United States diminished faster with epicentral distance than those earthquakes in the central and eastern U.S. of comparable size (Nuttli et al., 1979; Singh and Herrmann, 1983). Recent studies utilizing modern digital seismic instruments have confirmed that attenuation is noticeably higher, as much as six times, in the western United States (Mitchell, 1975; Frankel et al., 1990; Benz et al., 1997).

The acceptance of lateral heterogeneities within the crust has been widely acknowledged since the latter half of the previous century (Smithson, 1978; Christensen and Mooney, 1995). Therefore, Lg propagation is influenced by disparities in the crustal wave guide along its travel path. High attenuation has been suggested to be caused by several mechanisms, including highly fractured crust in tectonically active regions that effectively absorb high frequency seismic waves (Aki, 1980), elevated crustal temperatures (Frankel, 1991), and variations in crustal thickness and structures that control elastic wave propagation (Gregersen, 1984).

Lg appears as the dominant high-frequency phase in regional seismic waveforms, and is used extensively to determine a variety of effects that include earthquake-source parameters, site response, S-wave velocity, and attenuation (Atkinson and Mereu, 1992). Lg is generated by a superposition of higher-mode surface waves (Oliver and Ewing, 1957; Mitchell, 1975) or multiple reflected shear energy within the crustal waveguide (Gutenberg, 1955), which travel with a group velocity of about 3.5 km/sec. Since Lg loses energy quickly within transition zones where crustal thicknesses change drastically from either large to small or small to large, constant crustal thicknesses are needed to provide an effective waveguide (Kennett, 1986). In stable tectonic regions, such as North Africa, Lg has been observed at distances as great as 6000 km (McNamara and Walter, 2001), but in areas comparable to Northern California, Lg can be completely attenuated by local geology in less than 500 km.

Although there have been numerous studies to determine frequency-dependent Lg attenuation for the continental United States (Nuttli, 1973; Mitchell, 1975; Frankel, 1991; Benz et al., 1997), this is the first study to define Lg Q for three new regions and to incorporate a relatively large data set to produce a detailed Q map of the continental United States. In this article, we study the nature of Lg propagation and attenuation within seven regions of the continental United States. To accomplish this, seismic waveforms were first visually inspected for the presence of Lg amplitudes, and then Lg amplitudes were inverted for paths restricted to specific, predetermined tectonic regions. The frequency-dependent quality factor Q is commonly modeled using the power law in the form

$$Q(f) = Q_o (f / f_o)^{\eta},$$

where f_0 is a reference frequency ($f_0 = 1$ for this work), Q_0 is Q at the reference frequency, and η is assumed to be constant over the frequencies of interest.

DATA SELECTION

The Lg waveform data used in this study were acquired from January 2000 to February 2003 from local and regional earthquakes recorded by three component broadband stations of the U.S. National Seismic Network (USNSN), Global Seismic Network (GSN), Regional Seismic Network (RSN), and other cooperative stations which comprise the backbone of the Advanced National Seismic System (ANSS) (Table 1). Consistent processing and interpretation of the Lg attenuation results was made possible by the availability of high quality, calibrated waveforms from various regions of the United States, Canada, and Mexico which were fed in real time to the United States Geological Survey (USGS) at the National Earthquake Information Center (NEIC). The event locations were determined from the USGS's Preliminary Determination of Epicenter catalogue (PDE).

For our analysis, seven different regions across the continental United States were selected based on tectonic boundaries and ray path coverage. To reduce the trade off between source and receiver terms in the inversion, only station-event pairs were used that had a minimum of three observations. The three new regions that have not been previously studied for Lg Q include Northern California, the Pacific Northwest, and the Mountain States, while the previously studied regions are Southern California, the Basin and Range Province, the Central U.S., and the Northeastern United States.

Amplitude measurement of the Lg waveform is similar to the method utilized by McNamara et al. (2000) and Benz et al. (1997). Waveforms are visually inspected for the

presence of Lg on the vertical component at the appropriate time for a wave traveling at a typical continental Lg velocity (3.0 to 3.6 km/s) (McNamara et al., 1996). A qualitative analysis based on Signal to Noise Ratio (SNR) was then used to select Lg waveforms for the inversion. Instruments were deconvolved from velocity seismograms resulting in absolute ground displacement in meters. For each path, Lg amplitudes were measured in the frequency domain using a Root Mean Squares (RMS) technique on whole octaves for five passbands with center frequencies at 0.75, 1.5, 3.0, 6.0, and 12.0 Hz. For example, we measured a RMS over 2.0 to 4.0 Hz for the center frequency of 3.0 Hz to reduce the variance of amplitudes over whole octaves instead of measuring peak amplitudes which could be influenced by outliers. Lg was observed within a range of path lengths from several tens of kilometers to several thousand kilometers. Path lengths were limited to those greater than 110 kilometers because short epicentral distances made it difficult to determine the presence of Lg due to the interference of the local, faster S arrivals. Greater epicentral distances allowed the faster S waves to separate from the slower Lg waves, making it easier to distinguish between the two arrivals. Earthquake data was limited to those events greater than mb 3.5, and earthquake depths were restricted to less than 40 km to ensure that the Lg waves were generated and remained in the crust.

METHODS

The inversion technique used in this study to estimate the frequency dependence of Lg is described in detail by Benz et al. (1997) and McNamara et al. (1996).

The observed amplitude of Lg can be modeled as

$$A(f,D) = 1/D^{\gamma}\, R(f)S(f)e^{-\pi f D/vQ(f)}, \qquad (1)$$

where D is the hypocentral distance, _ is the exponent of the geometric spreading within the medium, R is the receiver term that denotes site effects, S is the term that represents the individual earthquake source excitation, f is the median frequency of the observed wave, v is the group velocity for Lg (3.5 km/s), and Q(f) is the quality factor of Lg propagation within the crust.

Rewriting and taking the natural log of both sides to linearize the above equation yields

$$\ln A(f) + \gamma \ln D = \ln R(f) + \ln S(f) - {\pi f D}/{vQ(f)}. \qquad (2)$$

When the left hand side of this equation is plotted against epicentral distance, the right hand side describes a line where the R and S terms control the intercept and the Q term controls the slope.

Since the response of most of our instruments are well known, it is possible to directly solve for the source and receiver terms along with the regional Q value by inverting instrument-corrected and geometrical spreading-corrected Lg amplitudes from many different events (Benz et al., 1997). With such a large data set of source-receiver pairs, it is possible to set up a system of linear equations based on equation (2). The system of equations can be expressed as

$$Ax = t, \qquad (3)$$

where **A** is the system matrix made up of the parameter coefficients of equation (2), **x** is a column vector containing the unknown event (S) and station (R) terms and the regional Q term, and the **t** vector is comprised of the left hand side of equation (2). The system matrix, **A**, is made up of mostly ones and zeros, with the last column listing a portion of

the last term of (2) $(\frac{-\pi f D}{v})$. By solving for each frequency independently, the known variables are f, D, and v for each source receiver pair. A singular value decomposition (SVD) inversion technique is then applied to determine the unknown variables, S, R, and Q, for each frequency in every region (e.g. Aster et al., 2002). As a test, a least squares inversion was also applied to the data which produced identical results to the SVD inversion.

The inversions were performed for five different whole octave frequency bands with center frequencies at 0.75, 1.5, 3.0, 6.0, and 12.0 Hz for each of the regions to obtain a unique measure of frequency-dependent Q(f). Since the effects of scattering or radiation pattern cannot be separated in this work, and a reasonable, constant geometric spreading rate is assumed, our results represent an apparent Q. Since Lg is a multiply reflected scattered wave that distributes energy across all three components of motion, radiation effects should be minimal (McNamara et al., 1996).

We made several assumptions in the Lg Q(f) computation. Based on the qualitative analysis of the data from the continental United States, we observed that the main Lg energy arrived within the group velocity window 3.6 to 3.1 km/s. A frequency-independent group velocity of 3.5 km/s was assumed based on this observation and the fact that Lg is not dispersive (Gutenberg, 1955).

An arbitrary reference station was selected to normalize the remaining stations. The reference station was chosen based on low background noise and well known response characteristics, but in the end, the choice of reference station had no effect on Q. Selection of a reference station is critical when determining relative receiver terms, but this topic is not discussed in this paper.

Since it is difficult to simultaneously solve for the geometric spreading and attenuation, the geometric spreading term, _, is assumed to remain constant at 0.5 for each region and frequency (Benz et al., 1997).

ERROR ANALYSIS

We examined the mean and standard deviation of Q for each region for all frequencies by resampling the original dataset using the delete-j Jackknife resampling technique modeled after the method of Efron and Tibshirani (1993). To achieve consistency for the Jackknife estimate of standard deviation, we left out at least d = $\sqrt{n}$, where n is the total number of observations and d is the number of observations removed from the complete dataset (Efron and Tibshirani, 1993). To obtain an error bound, we removed (d) number of randomly selected observations from the total (n) number of observations to create 1000 new Jackknife datasets, and then inverted each Jackknife dataset to determine 1000 Q values. From these 1000 Q values, we were able to calculate a standard deviation and mean value for the region at a desired frequency. We used 2 _ for our error bound and compared the mean Q to the actual Q computed from the entire dataset to test for stability and accuracy.

Figure 2 shows a histogram of the results obtained from 2000 different inversions of randomly selected Jackknife datasets from the Northern California region at 1.5 Hz. We used 2000 inversions for this example instead of the standard 1000 inversions to show that standard deviations do not change for more Jackknifed datasets and the distribution trends toward normal. We removed 10 different randomly selected observations from the complete dataset (n = 85) to create 2000 new Jackknife datasets, and then inverted each Jackknife dataset to obtain 2000 Q values.

The mean and standard deviation were calculated from this set of 2000 Q values to establish error estimates for the region. In this example, the complete dataset Q is 127 and the standard deviation is 2.6, therefore Q = 127 (±5) at 1.5 Hz. The distribution appears to be normal with a noticeable peak at about 127, which corresponds to both the Q calculated from the entire dataset and the mean Jackknife value of Q.

We also tested the stability of our datasets by removing an increasing amount of observations to determine where the data becomes unstable. The same dataset from above remained stable, with a standard deviation less than 30 and a delta Q less than 5, up until about 70% of the data was removed (Figure 3). This suggests that Q can be determined with relatively few observations, and that adding more observations merely decreases the error. This also reinforces our selection of tectonic regions in that Q is a reasonable estimate of the region average.

RESULTS

From the inversion results, we observe that tectonically stable regions such as the central United Sates generally have the highest Q_o values and the weakest frequency dependence (low _), while tectonically active regions generally have low Q_o values and high _ values.

SOUTHERN CALIFORNIA Figure 3A shows the distribution of broadband stations (triangles), earthquakes (circles), and source-receiver Lg paths (solid lines) for the Southern California region at 3 Hz. The maps were constructed at 3 Hz because this frequency represents the portion of the frequency band of interest with the best signal-to-noise ratio, thus providing a view of raypath coverage in each area. This region, ranging from 30°N to 37°N and 114°W to 122°W, includes the southern Coast Ranges, southern

Sierra Nevada, and a portion of the eastern Mojave and extensional region east of the Sierra Nevada, and is covered by 58 raypaths induced by 17 earthquakes and recorded at 5 stations. The focus here is to characterize the San Andreas Fault system. Several earthquakes and stations, such as the station on San Nicholas Island, were not used in this example because of noisy data and/or comparatively few spectral measurements.

Figure 3B shows a comparison of Lg spectral amplitude versus epicentral distance at center frequencies of 0.75, 1.5, 3.0, 6.0, and 12 Hz, corrected for source and receiver terms determined from the inversion. An L2 norm best-fit line was also applied to the corrected Lg amplitudes to show a linear trend in the data. The reference station for Southern California is TPNV, which is located in southwestern Nevada. The results show an increase in Lg Q from 141(±24) at 0.75 Hz to 1074(±92) at 12.0 Hz. The error terms, denoted by the plus and minus values, are 2 _ standard deviations computed from the Jackknife method described above. Generally, the standard deviation is relatively small at the middle frequencies (1.5, 3.0, and 6.0 Hz) and increases at the two end frequencies (0.75 and 12.0 Hz). This may be due to the fact that there are fewer raypaths at 12.0 Hz due to variation in instrumentation, and because of stronger effects of radiation pattern at lower frequencies which are not corrected for in the inversion (Benz et al., 1997). GSN stations record at 20 samples per second (Nyquist Frequency = 10 Hz), so it is impossible to sample true energy levels in the octave band ranging from 8 to 16 Hz with a center frequency of 12 Hz.

By plotting the Q values and error terms for each of the five frequencies on a log log scale, we see a frequency-dependent Q(f) function emerge (Figure 3C). We then fit a linear trend to the data using an L2 norm to produce a best fit frequency-dependent Lg Q

function of $Q(f) = 152(\pm 37)\ (f/1)^{0.72\ (\pm 0.16)}$ for the region. Our results vary slightly from Benz et al. (1997) who used similar inversion techniques, but fewer source-receiver raypaths to resolve a frequency-dependent Lg Q function of $Q(f) = 187(\pm 7)\ (f/1)^{0.55(\pm 0.03)}$ between 1.0 and 7.0 Hz. Our results are also consistent with the crustal coda Q results of Singh and Herrmann (1983) who find an average Q_o of 200 and _ of 0.6 for Southern California.

BASIN AND RANGE The Basin and Range Province is characterized by high heat flow and thin continental crust in a tectonically active environment. This region is mainly made up of Nevada and western Utah, but has several stations and/or events in southern Oregon, California, and Idaho. Figure 4A shows a map of the Basin and Range Province defined by the coordinates 36°N to 42.5°N and from 111°W to 120°W, with corresponding raypaths, stations, and earthquakes used in this study.

The Basin and Range Province is well sampled with 242 raypaths from 31 sources recorded by 17 stations. The best fit lines to the Lg spectral amplitudes, corrected for source and receiver terms, are shown in Figure 4B. DUG, located in west central Utah is used as the reference station. Results show that Lg Q increases from 183(±8) at 0.75 Hz to 1255(±54) at 12.0 Hz (Figure 4B).

Like Southern California, the Basin and Range Province shows a strong frequency dependent Lg Q with an equation of $Q(f) = 200(\pm 40)\ (f/1)^{0.68\ (\pm 0.12)}$ (Figure 4C). Chavez and Priestley (1986) also found similar results with a frequency-dependent Lg Q function of $Q(f) = 206\ f^{0.68}$ between the frequencies of 0.3 and 10.0 Hz with approximately 40 raypaths. Our Q function is also close to that determined by Benz et al. (1997) for their results between 1.0 and 5.0 Hz with $Q(f) = 235(\pm 11)\ (f/1)^{0.56(\pm 0.04)}$ for 90 raypaths. Coda

Q values presented by Xie and Mitchell (1990) are slightly different with a Q_c value of 267(±56) and a somewhat less frequency-dependent _ value of 0.37(±0.06). The east African rift is tectonically similar to the Basin and Range Province exhibiting active continental tectonics and a thin crust with a frequency-dependent Lg Q of $Q(f) = 186(\pm 7)\ f^{0.78(\pm 0.05)}$ (Ferdinand, 1998)

NORTHERN CALIFORNIA The Northern California region is defined by 85 raypaths from 18 earthquakes recorded at 7 stations, with coordinates of 37°N to 42°N and 119°W to 126°W (Figure 5A). This classic subduction zone region has no prior Lg Q results. Current attenuation numbers are necessary for hazard map mitigation in this densely populated area that has been subjected to large earthquakes. The best fit lines to the Lg spectral amplitudes, corrected for source and receiver terms, are shown in Figures 5B. We selected station BEKR for the reference station, which is located along the border of California and Nevada. Results show that Lg Q increases from 100(±5) at 0.75 Hz to 650(±22) at 12.0 Hz. Northern California has a best-fit frequency-dependent Lg Q function of $Q(f) = 105(\pm 26)\ (f/1)^{0.67\ (\pm 0.16)}$ (Figure 5C).

PACIFIC NORTHWEST The Pacific Northwest region is made up of Washington, Oregon, western Idaho and northern California and Nevada, and contains 16 earthquakes producing 90 raypaths at 12 stations (Figure 6A). Figure 6B shows a best fit linear approximation for the Lg spectral amplitude of five octaves corrected for receiver and source terms. The northeast corner of California contains the reference station MOD for this inversion. Values of Q increase from 148(±8) to 1233(±68) for the frequencies of 0.75 to 12.0 Hz.

The Pacific Northwest also has a low Q_o value and a large frequency dependency with an equation of $Q(f) = 152(\pm 49)\ (f/1)^{0.76\ (\pm 0.18)}$ (Figure 6C). The tectonic setting and the frequency-dependent function are both similar to the Northern California region. Since there are no previous Lg Q studies in this area, a comparison to a similar tectonic region in south-central Alaska is required, which produced a frequency-dependent quality factor of $Q(f) = 220(\pm 30)\ f^{0.66(\pm 0.09)}$ (McNamara, 2000).

MOUNTAIN STATES The Northern Mountain States are western Montana and Wyoming and eastern Idaho, and are well covered with 195 raypaths caused by 34 earthquakes and recorded by 10 stations (Figure 7A). This area is centered on the tectonically active Yellowstone hotspot in northwestern Wyoming and does not have a previously determined Q(f) function.

The equation for the frequency dependent Q for the Northern Mountain states is $Q(f) = 166(\pm 37)\ (f/1)^{0.61\ (\pm 0.14)}$ (Figure 7C) Results show that Lg Q increases from 163(±11) at 0.75 Hz to 862(±50) at 12.0 Hz (Figure 7B).

CENTRAL USA Figures 8A-C show a map and results for the Central United States area located in the Midwest continental United States with coordinates 32°N to 40°N and from 82°W to 103°W. This is a tectonically stable region with an active fault (New Madrid) that is well covered with 156 raypaths from 22 earthquakes recorded at 16 broadband stations. Q values for the New Madrid area are much higher than those of the western U.S. regions presented above with Q values increasing from $635^{\pm 38}$ at 1.5 Hz to $1865^{\pm 64}$ at 12.0 Hz. WMOK was used as the reference station, and is located in southwestern Oklahoma. The equation for the best fit linear approximation to the data is

$Q(f) = 640(\pm 225)\ (f/1)^{0.344\ (\pm 0.22)}$, which reinforces our hypothesis of high a Q_o value and a low _ value for regions that are tectonically stable.

The Q value at 0.75 Hz appears to be an anomaly in this region, so we removed it and recalculated the Lg Q function (Figure 8C). Between 1.0 and 12.0 Hz, the Lg Q function is $Q(f) = 470(\pm 127)\ (f/1)^{0.52\ (\pm 0.16)}$. The Q_o error termed decreased from 225 to 127 and the _ error term decreased from 0.22 to 0.16. A non frequency-dependent Lg Q was presented by Benz et al. (1997) with a mean Q value of 1291, while Singh and Herrmann (1983) found Q_o to vary from 900 to 1350 at 1 Hz with a small frequency dependence described by _ = 0.1 to 0.3. Our results are noticeably lower than other studies in the Central United States, but we were able to find a frequency-dependent Lg Q.

NORTHEAST USA Northeastern United States is a typical intraplate region with moderate seismicity (mb usually less than 4.5), characterized by scattered epicenters (Shi et al., 1996). This region can be seen in Figure 9A represented by 12 earthquakes recorded at 12 stations for a total of 70 raypaths.

Results show Lg Q increasing from 676(±170) at 0.75 Hz to 1843(±130) at 12.0 Hz (Figure 17). Large Jackknife standard deviations reinforce our hypothesis that station instrumentation might vary over time without our knowledge. Station NCB was chosen for the reference station, and is located in upstate New York. The linear equation that best represents our data on a log log plot is $Q(f) = 650(\pm 143)\ (f/1)^{0.36\ (\pm 0.14)}$ (Figure 9C). Shi et al. (1996) found an average frequency-dependent Q_o of 723 and an average _ of 0.42 for a region similar to the one used in this study.

DISCUSSION

Southern and Northern California, the Pacific Northwest, the Mountain States, and the Basin and Range Province are all well described by low Lg Q and strong frequency dependence, while the Central and Northeastern United States are best described by high Lg Q and weak frequency dependence (Figure 10). Furthermore, Lg Q exhibits a minimum between 0.75 and 1.5 Hz and increases in value up to 12.0 Hz for all seven regions studied in this paper. A comparison of Lg amplitude decay in the seven different regions reinforces our findings since amplitudes decay much faster in the western U.S. versus the decay rate in the eastern United States (Figure 11).

Although the linear fits to the Lg amplitudes are good, the Central and Northeastern U.S. regions have the largest standard deviations of the seven regions. Raypath coverage is not an issue for the Central U.S. since this region has over 150 raypaths. Various smaller regions centered around the New Madrid fault were inverted for Lg Q to test for stability, but we found higher standard deviations with similar Lg Q values. High frequency surface wave contamination might be responsible for the relatively high variation in standard deviation for this region.

The Northeast U.S. region has less than half the raypaths of the central U.S. with only 70 raypaths covering this region. Not all stations in this area are maintained by the USGS, therefore we lack sufficient information to properly identify the response on these broadband stations. Consequently, high standard deviations might be caused by any one or a combination of surface wave contamination, raypath coverage, or unknown instrument response. Shi et al. (1996) divided this region into three sub regions consisting of the Adirondack Mountains ($Q = 905\ f^{0.40}$), the central Appalachian Province ($Q = 561\text{-}586\ f^{0.46\text{-}0.47}$, and northern New England Appalachians ($Q = 705\ f^{0.41}$).

Our frequency-dependent function falls roughly in the middle of their results with a value of $Q(f) = 650^{\pm 143} (f/1)^{0.36\ (\pm 0.14)}$. The variation in results is probably due to different raypaths and coverage density.

The Pacific Northwest and the Northern California region have not been extensively studied in the past for Lg Q, but similar results to other comparable tectonic regions, such as south-central Alaska, support our results. The Mountain States region is influenced by the high attenuation of the Yellowstone hotspot, and has not been recently studied with this kind of raypath coverage. The remaining two regions (Southern California and the Basin and Range Province) all exhibit frequency-dependent Lg functions that are similar to precious studies.

CONCLUSION

Our objective in this article was to document differences in Lg attenuation between seven different tectonic regions in the continental United States. Standardized instrumentation and consistent processing provide attenuation functions that can be used in a variety of applications including local magnitude estimates, earthquake hazard assessment in populated areas, and structural engineering applications. Further work will include obtaining more data to determine Lg Q for the remaining tectonic areas of the U.S., and to expand the technique to a 2 D tomographic inversion of the entire continental United States.

REFERENCES

Aki, K., Scattering and Attenuation of Shear Waves in the Lithosphere, J. Geophys. Res., 85, 6496-6504, 1980.

Aster, R., Borchers, B., and Thurber, W., Parameter Estimation and Inverse Problems, 2002.

Atkinson, G. and Mereu, R., The Shape of Ground Motion Attenuation Curves in Southeastern Canada, Bull. Seism. Soc. Am., 82, 2014-2031, 1992.

Benz, H., Frankel, A., and Boore, D., Regional Lg Attenuation of the Continental United States, Bull. Seism. Soc. Am, 87, 606-619, 1997.

Chavez, D. and Priestley, K., Measurement of Frequency Dependent Lg Attenuation in the Great Basin, Geophys. Res. Lett., 13, 551-554, 1986.

Christensen, N. and Mooney, W., Seismic velocity structure and composition of the continental crust: A global view, J. Geophys. Res., 100, 9761-9788, 1995.

Efron and Tibshirani, An introduction to the Bootstrap, Monographs on Statistics and Applied Probability, 57, 1993.

Ferdinand, R.W., Average attenuation of 0.7-5.0 Hz Lg waves and magnitude scale determination for the region bounding the western branch of the East African Rift, Geophys. J. Int., 134, 818-830, 1998.

Frankel, A., Mechanisms of Seismic Attenuation in the Crust: Scattering and Anelasticity in New York State, South Africa, and Southern California, J. Geophys. Res. Research, 96, 6269-6289, 1991.

Gregersen, S., Lg-wave propagation and crustal structure differences near Denmark and the North Sea, Geophys. J. R. Astr. Soc., 79, 217-234, 1984.

Gutenberg, B., Channel waves in the Earth's crust, Geophysics, 20, 283-294, 1955.

Herrmann, R. and A. Kijko, Modeling some empirical vertical component Lg relations, Bull. Seism. Soc. Am. 73, 157-171, 1983.

Kennett, B., Lg waves and structural boundaries, Bull Seism. Soc. Am., 76, 1133-1141, 1986.

McNamara, D. and W. Walter, Mapping crustal heterogeneity using Lg propagation efficiency throughoutthe Middle East, Mediterranean, Southern Europe and Northern Africa, PAGEOPH, 158, 1165-1188, 2001.

McNamara, D.E., Frequency Dependent Lg Attenuation in South-Central Alaska, Geophys. Res. Lett., 27, 3949-3952, 2000.

McNamara, D.E., Owens, T.J., and Walter, W.R., Propagation Characteristics of Lg across the Tibetan Plateau, Bull. Seism. Soc. Am, 86, 457-469, 1996.

Mitchell, B., Regional Rayleigh Wave Attenuation in North America, J. Geophys. Res., 80, 4904-4916, 1975.

Mitchell, B., Regional Variation and Frequency Dependence of QB in the Crust of the United States, Bull. Seism. Soc. Am, 71, 1531-1538, 1981.

Nuttli, O., Seismic Wave Attenuation and Magnitude Relations for Eastern North America, J. Geophys. Res., 78, 876-885, 1973.

Oliver, J. and Ewing, M., Higher Modes of Continental Rayleigh Waves, Bull. Seism. Soc. Am, 47, 187-204, 1957.

Press, F. and Ewing, M., Two Slow Surface Waves Across North America, Bull. Seism. Soc. Am, 42, 219-228, 1952.

Reese, C.C., Rapine, R.R., Ni, J.F., Lateral Variation of Pn and Lg Attenuation at the CDSN Station LSA, Bull. Seism. Soc. Am, 89, 325-330, 1999.
Shi, J., Kim, W., and Richards, P., Variability of crustal attenuation in the northeastern United States from Lg waves, J. Geophys. Res., 101, 25,231-25,242, 1996.
Singh, S. and Herrmann, R., Regionalization of Crustal Coda Q in the Continental United States, J. Geophys. Res., 88, 527-538, 1983.
Smithson, S., Modeling Continental Crust: Structural and Chemical Constraints, Geophys. Res. Lett., 9, 749-752, 1978.
Xie, J. K. and Mitchell, B.J., Attenuation of multiphase surface waves in the Basin and Range province, part I: Lg and Lg coda, Geophys. J. Int., 102, 121-137, 1990.

FIGURE CAPTIONS

Table 1. Table listing seismic stations, locations, number of recorded earthquakes, and region(s) were station was located for this experiment.

Figure 1. Histogram of 2000 Jackknife Q inversions for Northern California region at 1.5 Hz. In this example, total number of observations (n) = 85 and number of observations removed for each Jackknife inversion (d) = 10. Note normal distribution of Q values. Actual Q value is 127.4, Average Jackknife Q value is 127.5, with a difference of only 0.1.

Figure 2. Plot a) shows the difference between the average Jackknife Q and the actual Q value versus the percent of data removed from the original dataset before inverting for Q. Note dataset is relatively stable up until about 70 percent of the data is removed. Plot b) shows the standard deviation versus percent of data removed from the original dataset before inversion. Note standard deviation also remains low and stable up until about 70 percent of the original data is removed.

Figure 3. A) Map of Southern California study area sampled at 3 Hz. Triangles are broadband stations, circles are events, and lines represent station-receiver Lg raypaths used in this region. This area is covered by 58 raypaths from 17 earthquakes recorded at 5 stations. 30°N to 37°N and 114°W to 122°W define this region. B) Southern California Lg spectral amplitudes (dots) at 0.75, 1.5, 3.0, 6.0, and 12.0 Hz, corrected for source and receiver terms. Solid line is a best fit linear trend for data assuming frequency-independent Q and a _ of 0.5. Plus and minus terms for Q are derived from the standard deviation of the Jackknife method described above and equate to 2 _. C) shows the 5 values of Lg for each center frequency with corresponding error bars plotted on a log log graph to exhibit the linear frequency dependence of the Southern California region. The best fit frequency-dependent Lg Q function is $Q(f) = 152^{\pm 37} (f/1)^{0.72 (\pm 0.16)}$, where the plus and minus terms are the error terms for the best fit line.

Figure 4. A) Basin and Range province sampled at 3 Hz. Triangles are broadband stations, circles are events, and lines represent Lg source-receiver raypaths used in this study. This area is covered by 242 raypaths, 31 earthquakes, and 17 stations. The coordinates for this province are 36°N to 42.5°N and from 111°W to 120°W. B) Basin and Range Province Lg spectral amplitudes (dots) at 0.75, 1.5, 3.0, 6.0, and 12.0 Hz, corrected for source and receiver terms. Solid line is best fit linear trend for data assuming frequency-independent Q and a _ of 0.5. Graph C contains the five values for Q at each center frequency with corresponding error bars and a best fit linear trend plotted on a log log graph to show a frequency-dependent Q. The best-fit frequency-dependent Lg Q function is $Q(f) = 200^{\pm 40} (f/1)^{0.679 (\pm 0.12)}$ between 0.75 and 12.0 Hz.

Figure 5. A) Northern California region ranges from 37°N to 42°N and from 119°W to 126°W. Triangles are broadband stations, circles are events, and lines represent Lg paths use in this study. There are 85 raypaths, 18 earthquakes, and 7 stations in this 3 Hz sample region. B) Northern California Lg spectral amplitudes and corresponding best fit

lines that have been corrected for source and receiver terms. Best fit line assumes a frequency independent Q and a _ of 0.5. C) The log log graph f shows a frequency-dependent Lg Q for the Northern California region with a best fit function of $Q(f) = 105^{\pm 26} (f/1)^{0.67 (\pm 0.16)}$ between 0.75 and 12.0 Hz.

Figure 6. A) Pacific Northwest raypath map at 3 Hz. This region ranges from 40°N to 50°N and 113°W to 126°W, and contains 90 raypaths from 16 earthquakes recorded at 12 stations. Triangles, circles, and lines represent stations, earthquakes, and source-receiver raypaths respectively. B) Results for Pacific Northwest showing Lg amplitudes for 5 different center frequencies and matching best fit linear approximation assuming frequency-independent Q and a _ = 0.5. Plot C shows the best-fit frequency-dependent Lg Q function of $Q(f) = 152^{\pm 49} (f/1)^{0.761 \pm 0.18)}$.

Figure 7. A) Raypath map for the Mountain States region with coordinates of 41°N to 50°N and 105°W to 117°W. This region is covered by 195 raypaths from 34 earthquakes recorded at 10 stations at 3 Hz. B) The Mountain States region results for the center frequencies of 0.75, 1.5, 3.0, 6.0 and 12.0 Hz. The solid line represents the best fit linear approximation assuming a frequency-independent Q and a _ = 0.5. Graph C shows the corresponding Q values plotted on a log log scale with matching error bars and a best-fit frequency-dependent Lg Q function of $Q(f) = 166^{\pm 37} (f/1)^{0.61 (\pm 0.14)}$ between 0.75 and 12.0 Hz.

Figure 8. A) Path map for Central United States with 156 raypaths, 22 earthquakes, and 16 stations. This region is defined by the coordinates 32°N to 40°N and from 82°W to 103°W. B) Central United States results showing Lg amplitudes corrected for receiver and source terms. The solid line is a L2 norm linear approximation assuming a frequency-independent Q and a _ = 0.5. Graph C is a log log chart showing the values for Q at each frequency with matching errors and three best fit lines. The Q terms on either end have a large error, so we fit 3 lines, one with all five frequencies included, one with the 0.75 Hz Q value removed, and one with the 12.0 Hz term removed. The frequency-dependent Lg Q function for this region using all five Q values is $Q(f) = 640^{\pm 225} (f/1)^{0.344 (\pm 0.22)}$. $Q(f) = 470^{\pm 127} (f/1)^{0.52(\pm 0.16)}$ for the frequency-dependent function with 0.75 Hz Q removed. And with the 12.0 Hz value removed, $Q(f) = 683 (f/1)^{0.19}$.

Figure 9. Northeast United States region raypath coverage map at 3 Hz. Solid lines indicate source-receiver raypaths, circles represent earthquakes, and triangles symbolize stations. This region is limited to the coordinates of 37°N to 45°N and 68°W to 80°W, and defined by 70 raypaths from 12 earthquakes recorded at 12 stations. B) Northeast United States Lg spectral amplitudes (dots) at 0.75, 1.5, 3.0, 6.0, and 12.0 Hz, corrected for source and receiver terms. Solid line is best fit linear trend for data assuming frequency-independent Q and a _ of 0.5. Graph C contains the five values for Q at each center frequency with corresponding error bars and a best fit linear trend plotted on a log log graph to show a frequency-dependent Q. The best-fit frequency-dependent Lg Q function is $Q(f) = 650^{+/-143} (f/1)^{0.36 (+/-0.14)}$ between 0.75 and 12.0 Hz.

Figure 10. Log log graph showing all regions described above. Notice steeper slope and lower Q values for the active tectonic regions in the western United States versus the flatter slopes and higher Q values of central and northeastern United States.

Figure 11. Q values for the seven different regions presented above shown on a map of the continental United States for each of the five center frequencies (0.75, 1.5, 3.0, 6.0, and 12.0 Hz). Red denotes low Q values and blue represents high Q values.

Station Location List

Station	Latitude	Longitude	No. Observations	Region
AHID	42.7654	-111.1004	44	Mtn States
BEKR	39.8667	-120.3586	40	N. California
BINY	42.199	-75.986	28	NE USA
BLO	39.172	-86.522	12	Central USA
BMN	40.4314	-117.2217	39	Basin & Range/Pacific NW
BOZ	45.5999	-111.1633	46	Mtn States
BRYW	41.918	-71.539	1	NE USA
BW06	42.7777	-109.5555	53	Mtn States
CBKS	38.814	-99.7373	33	Central USA
CBN	38.205	-77.373	6	NE USA
CCM	38.0556	-91.2445	27	Central USA
CMB	38.035	-120.385	57	N. California
COR	44.5857	-123.3031	11	Pacific NW
CTU	40.6925	-111.7503	28	Basin & Range
DAC	36.277	-117.5937	33	S. California/Basin & Range
DUG	40.195	-112.8133	65	Basin & Range
ELK	40.7448	-115.2387	56	Basin & Range/Pacific NW
GNAR	35.965	-90.018	4	Central USA
GOGA	33.411	-83.467	18	Central USA
GWDE	38.826	-75.617	7	NE USA
HAWA	46.3925	-119.5323	37	Pacific NW
HLID	43.563	-114.414	71	Pacific NW/Mtn States
HNH	43.705	-72.286	10	NE USA
HOPS	38.994	-123.072	18	N. California
HRV	42.506	-71.558	12	NE USA
HVU	41.78	-112.775	53	Basin & Range/Mtn States
HWUT	41.6073	-111.565	71	Basin & Range/Mtn States
ISA	35.6633	-118.4733	52	S. California
KNB	37.0166	-112.8224	26	Basin & Range
LBNH	44.24	-71.926	24	NE USA
LKWY	44.5651	-110.4	33	Mtn States
LRAL	33.035	-86.998	11	Central USA
LSCT	41.678	-73.224	20	NE USA
MCWV	39.6581	-79.8456	17	NE USA
MIAR	34.5457	-93.573	31	Central USA
MNV	38.4328	-118.1531	58	Basin & Range
MOD	41.9033	-120.3058	40	N. California/Pacific NW
MPU	40.016	-111.63	20	Basin & Range
MSO	46.8292	-113.9406	24	Pacific NW/Mtn States
MVU	38.504	-112.21	32	Basin & Range
MYNC	35.074	-84.128	9	Central USA
NCB	43.971	-74.224	24	NE USA
NEW	48.2633	-117.12	42	Pacific NW
NOQ	40.653	-112.12	10	Basin & Range
OCWA	47.749	-124.178	10	Pacific NW
OXF	34.512	-89.409	28	Central USA
PAHR	39.7065	-119.3841	15	Basin & Range/N. California
PAL	41.006	-73.908	22	Central USA/NE USA
PAS	34.148	-118.17	6	S. California
PFO	33.6091	-116.4552	32	S. California
PGC	48.65	-123.45	3	Pacific NW
SAO	36.765	-121.445	39	S. California

SIUC	37.715	-89.218	18	Central USA
SLM	38.636	-90.236	6	Central USA
SNCC	33.248	-119.524	2	S. California
SPW	47.554	-122.25	1	Pacific NW
SSPA	40.636	-77.888	23	NE USA
SWET	35.216	-85.932	3	Central USA
TPH	38.075	-117.2225	53	Basin & Range
TPNV	36.9286	-116.2236	77	S. California/Basin & Range
UALR	34.775	-92.344	7	Central USA
VTV	34.567	-117.33	1	S. California
WALA	49.058	-113.92	20	Pacific NW/Mtn States
WCI	38.229	-86.294	23	Central USA
WCN	39.3106	-119.7563	34	Basin & Range/N. California
WDC	40.58	-122.5397	29	N. California/Pacific NW
WES	42.385	-71.322	3	NE USA
WMOK	34.738	-98.781	36	Central USA
WVL	44.565	-69.658	5	NE USA
WVOR	42.4339	-118.6367	34	Basin & Range/Pacific NW
WVT	36.13	-87.83	27	Central USA
YBH	41.7318	-122.7105	20	N. California/Pacific NW
YMR	44.669	-110.97	22	Mtn States

Table 1

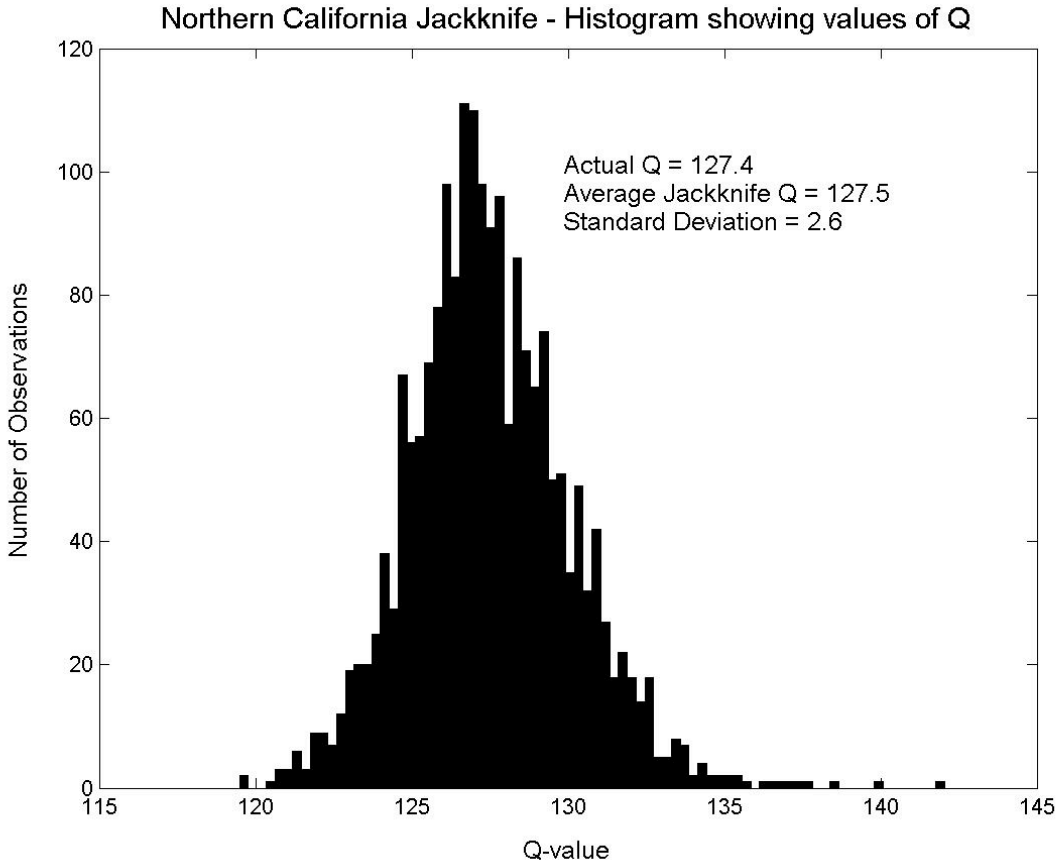
Northern California Jackknife - Histogram showing values of Q
Actual Q = 127.4
Average Jackknife Q = 127.5
Standard Deviation = 2.6
Number of Observations
Q-value
0
20
40
60
80
100
120
115
120
125
130
135
140
145

Figure 1

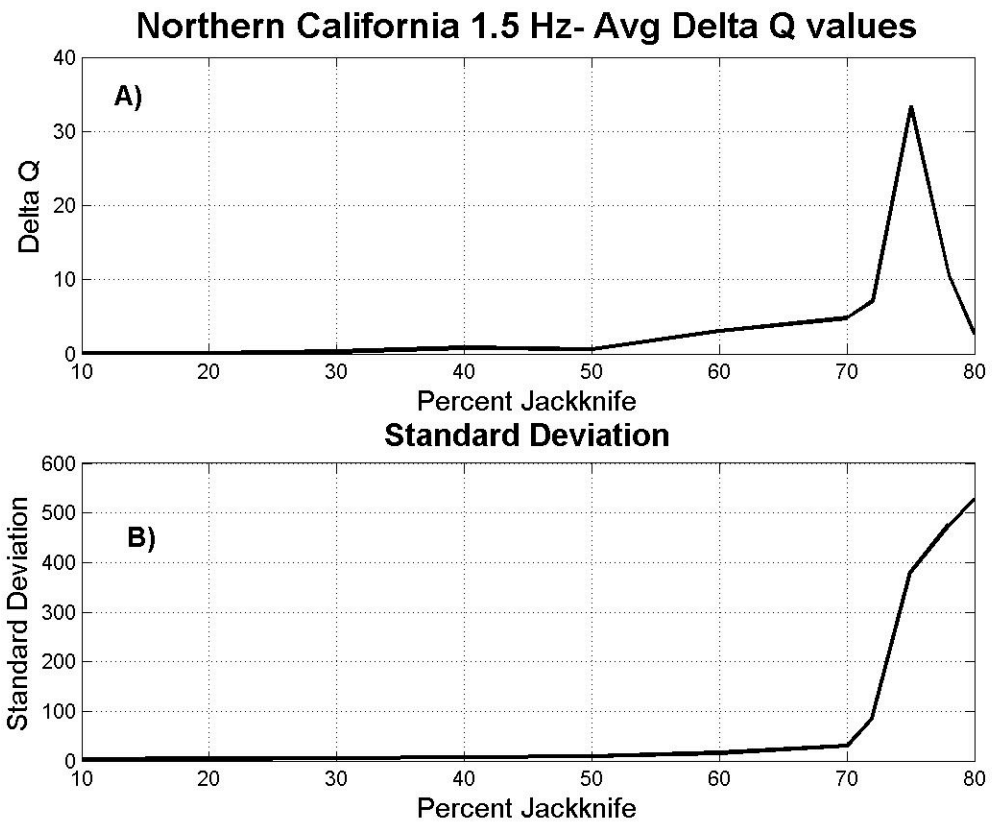
Northern California 1.5 Hz- Avg Delta Q values
A)
Delta Q
Percent Jackknife
Standard Deviation
B)
Standard Deviation
Percent Jackknife

Figure 2

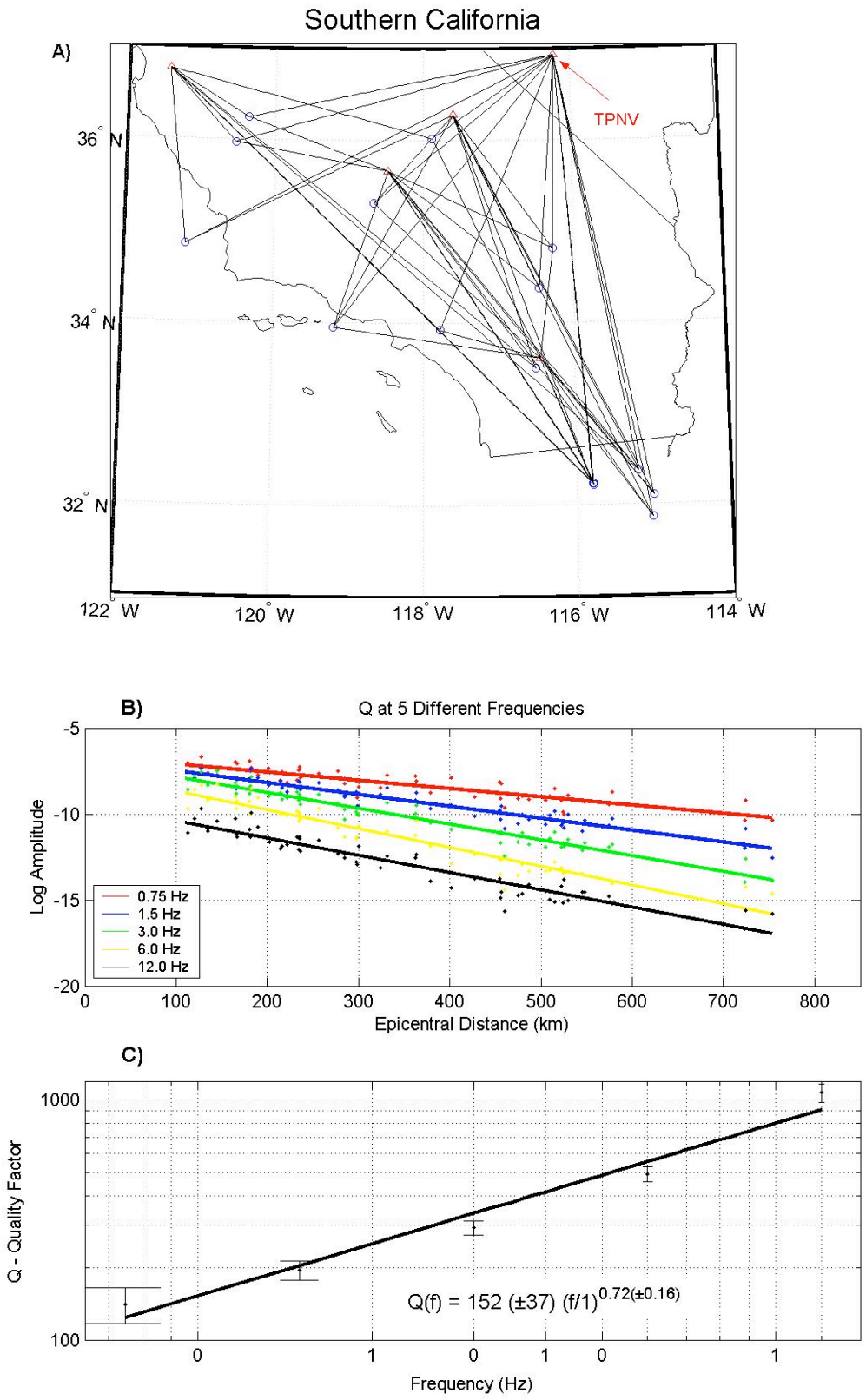
Southern California
A)
TPNV
36° N
34° N
32° N
122° W
120° W
118° W
116° W
114° W
B)
Q at 5 Different Frequencies
Log Amplitude
-5
-10
-15
-20
0.75 Hz
1.5 Hz
3.0 Hz
6.0 Hz
12.0 Hz
0
100
200
300
400
500
600
700
800
Epicentral Distance (km)
C)
Q - Quality Factor
1000
100
Q(f) = 152 (±37) (f/1)^0.72(±0.16)
0
1
0
1
0
1
Frequency (Hz)

Figure 3

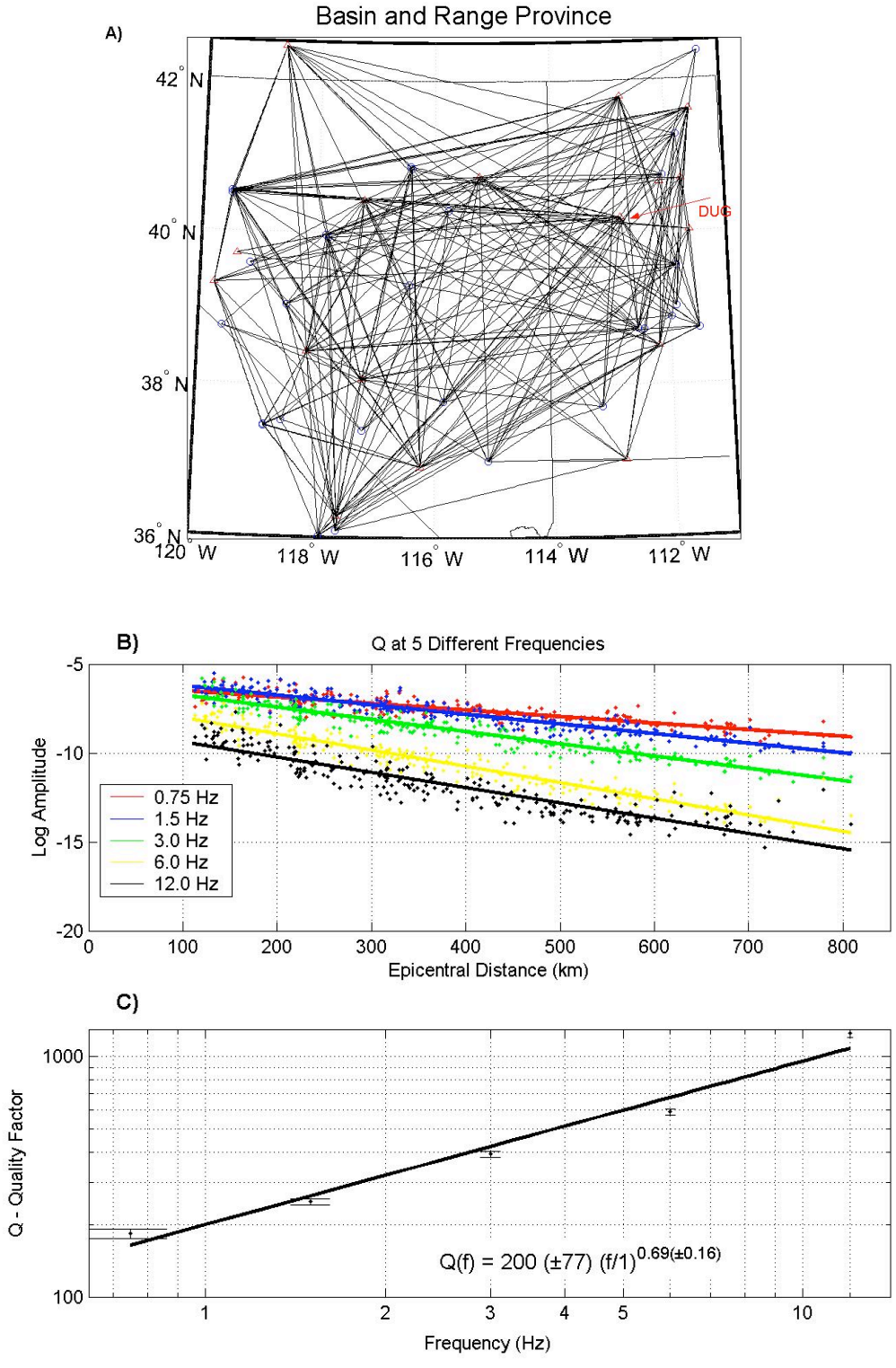
A)
Basin and Range Province
42° N
40° N
38° N
36° N
120° W
118° W
116° W
114° W
112° W
DUG
B)
Q at 5 Different Frequencies
Log Amplitude
Epicentral Distance (km)
0.75 Hz
1.5 Hz
3.0 Hz
6.0 Hz
12.0 Hz
C)
Q - Quality Factor
Frequency (Hz)
Q(f) = 200 (±77) (f/1)^0.69(±0.16)

Figure 4

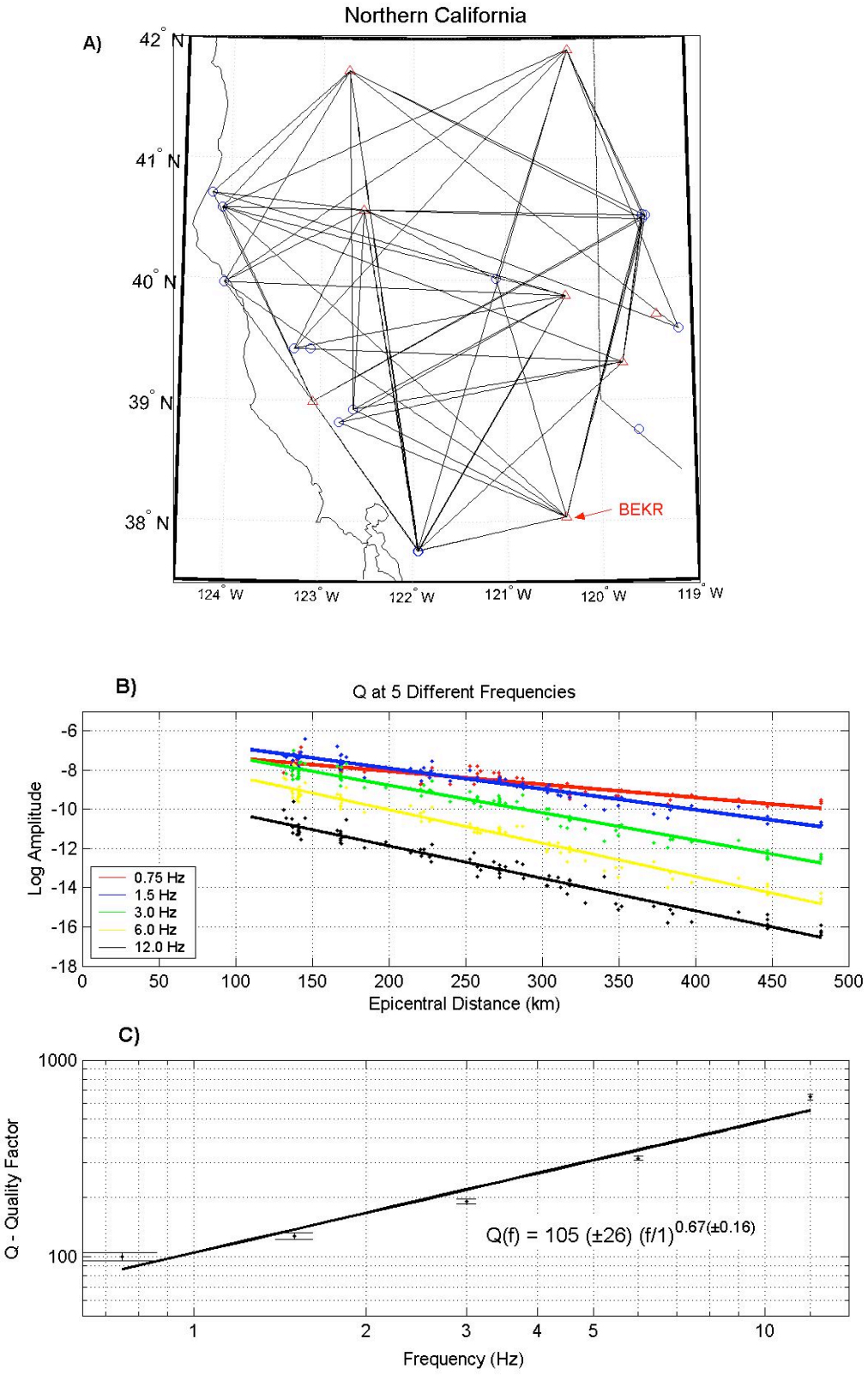
A)
Northern California
42° N
41° N
40° N
39° N
38° N
124° W
123° W
122° W
121° W
120° W
119° W
BEKR
B)
Q at 5 Different Frequencies
Log Amplitude
Epicentral Distance (km)
0.75 Hz
1.5 Hz
3.0 Hz
6.0 Hz
12.0 Hz
C)
Q - Quality Factor
Frequency (Hz)
Q(f) = 105 (±26) (f/1)^0.67(±0.16)

Figure 5

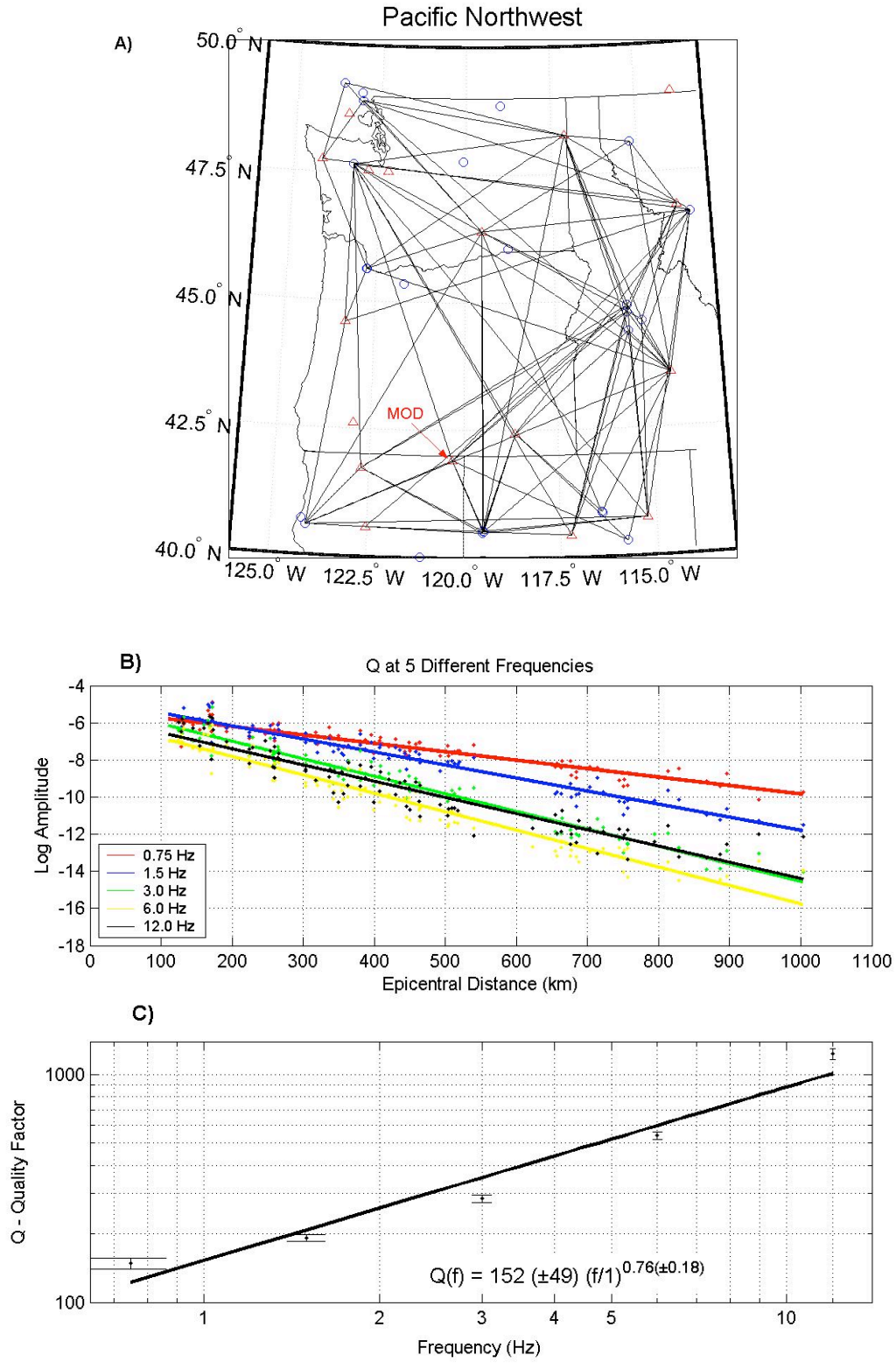
A)
Pacific Northwest
50.0° N
47.5° N
45.0° N
42.5° N
40.0° N
125.0° W
122.5° W
120.0° W
117.5° W
115.0° W
MOD
B)
Q at 5 Different Frequencies
Log Amplitude
0.75 Hz
1.5 Hz
3.0 Hz
6.0 Hz
12.0 Hz
Epicentral Distance (km)
C)
Q - Quality Factor
Q(f) = 152 (±49) (f/1)^0.76(±0.18)
Frequency (Hz)

Figure 6

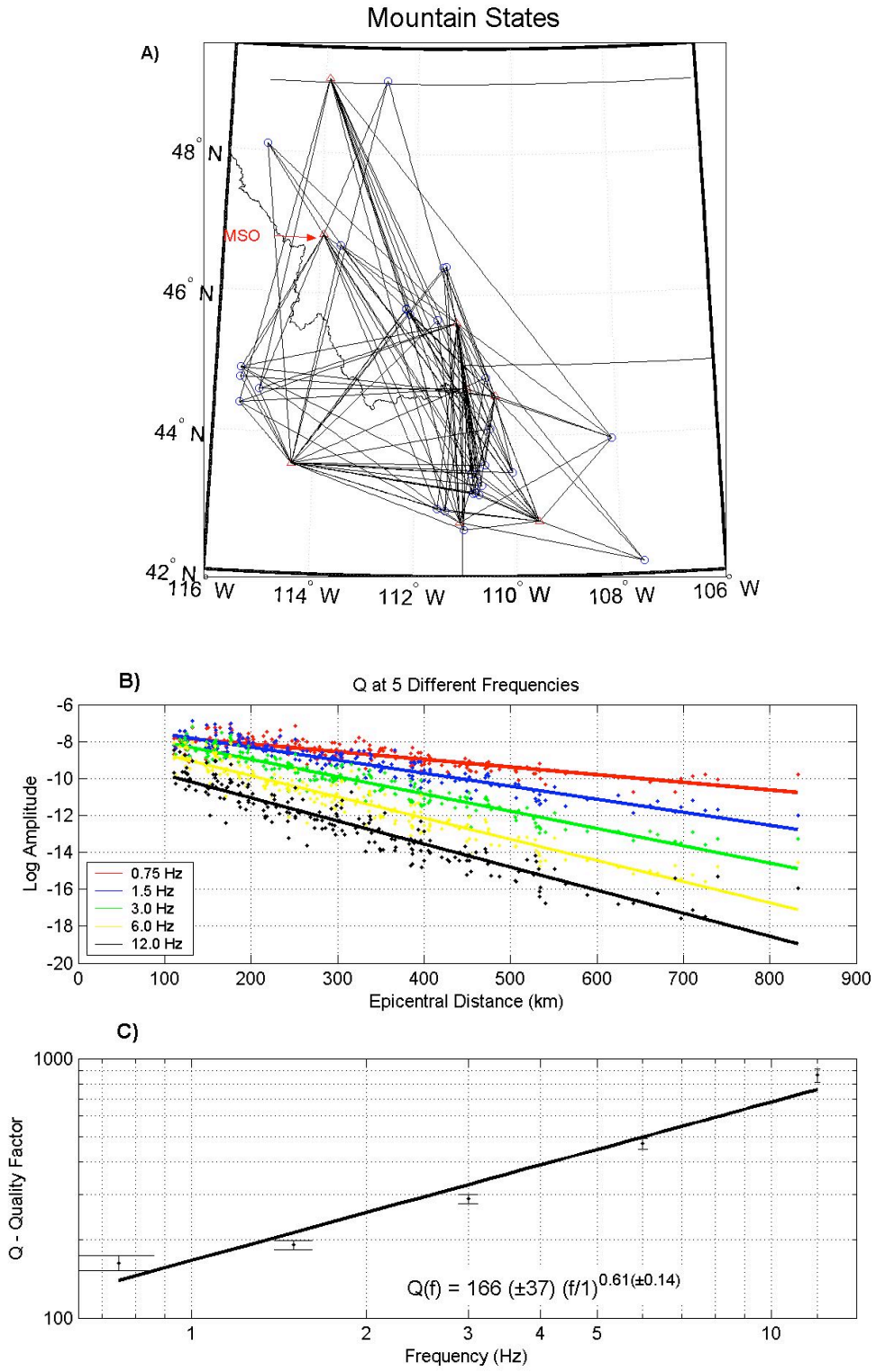
Mountain States
A)
48° N
46° N
44° N
42° N
MSO
116° W
114° W
112° W
110° W
108° W
106° W
B)
Q at 5 Different Frequencies
Log Amplitude
0.75 Hz
1.5 Hz
3.0 Hz
6.0 Hz
12.0 Hz
Epicentral Distance (km)
C)
Q - Quality Factor
Q(f) = 166 (±37) (f/1)^0.61(±0.14)
Frequency (Hz)

Figure 7

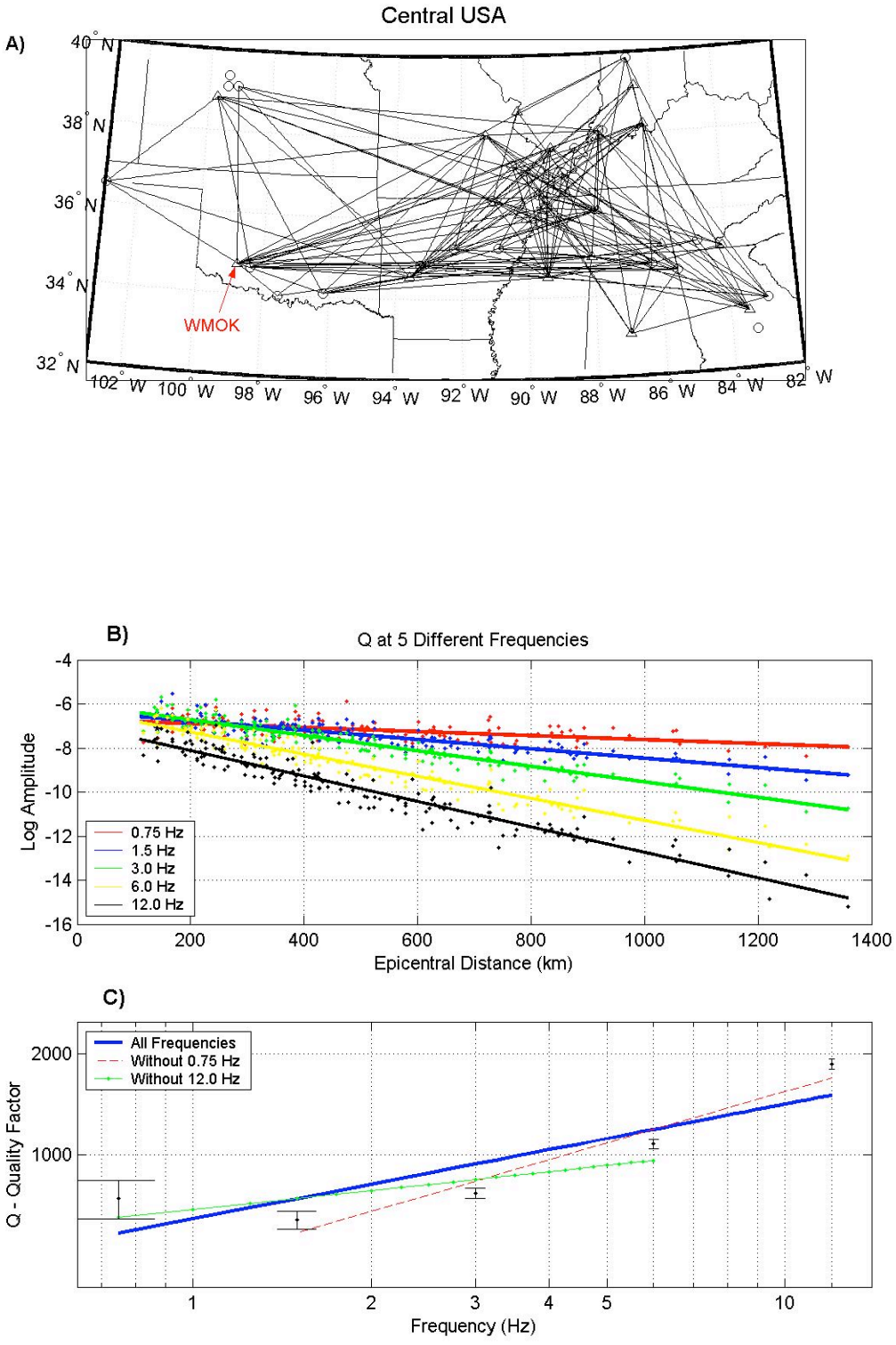
A)
Central USA
40° N
38° N
36° N
34° N
32° N
WMOK
102° W
100° W
98° W
96° W
94° W
92° W
90° W
88° W
86° W
84° W
82° W
B)
Q at 5 Different Frequencies
Log Amplitude
0.75 Hz
1.5 Hz
3.0 Hz
6.0 Hz
12.0 Hz
Epicentral Distance (km)
C)
All Frequencies
Without 0.75 Hz
Without 12.0 Hz
Q - Quality Factor
Frequency (Hz)

Figure 8

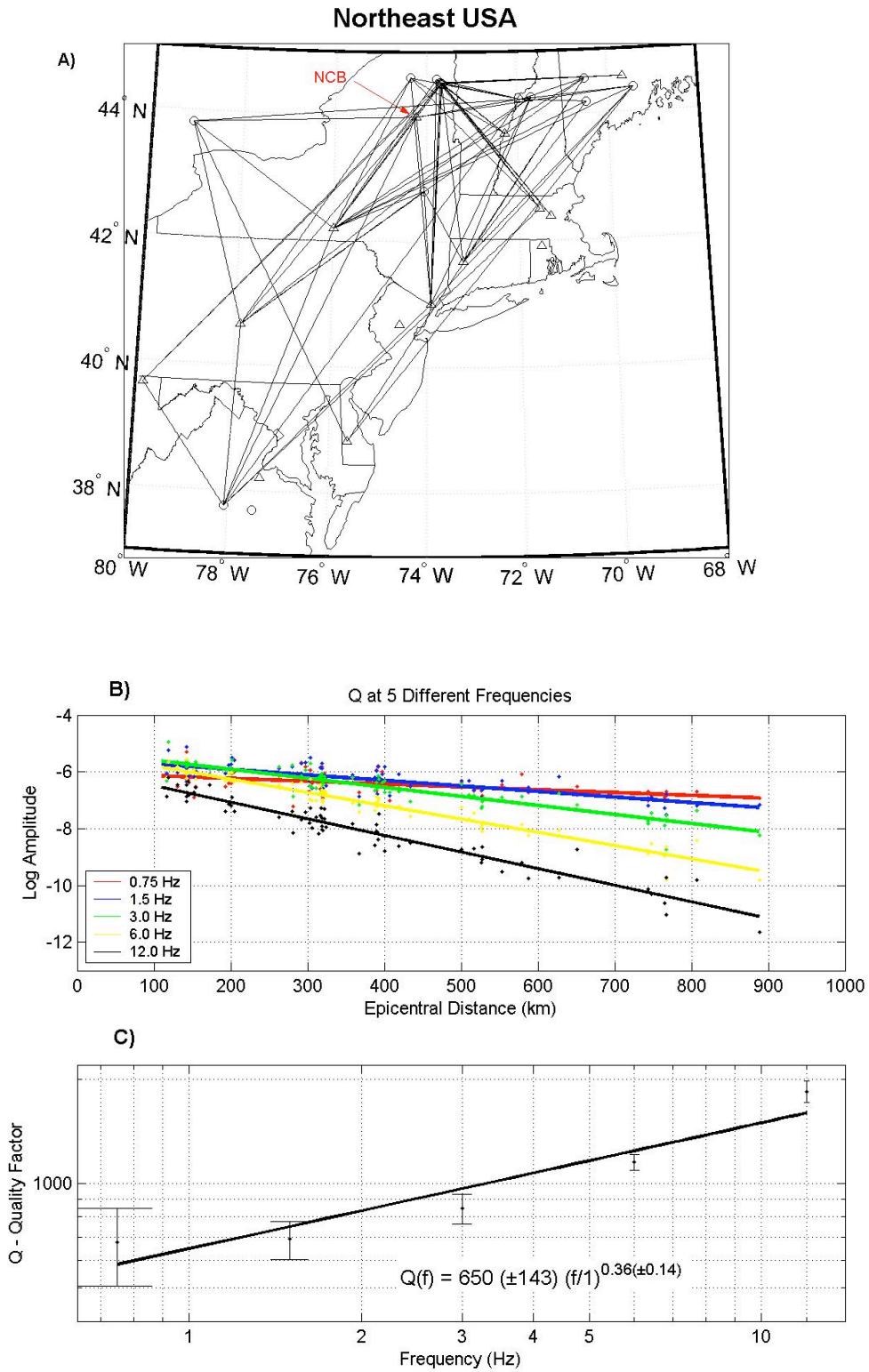
Northeast USA
A)
NCB
44° N
42° N
40° N
38° N
80° W
78° W
76° W
74° W
72° W
70° W
68° W
B)
Q at 5 Different Frequencies
Log Amplitude
0.75 Hz
1.5 Hz
3.0 Hz
6.0 Hz
12.0 Hz
Epicentral Distance (km)
C)
Q - Quality Factor
Q(f) = 650 (±143) (f/1)^0.36(±0.14)
Frequency (Hz)

Figure 9

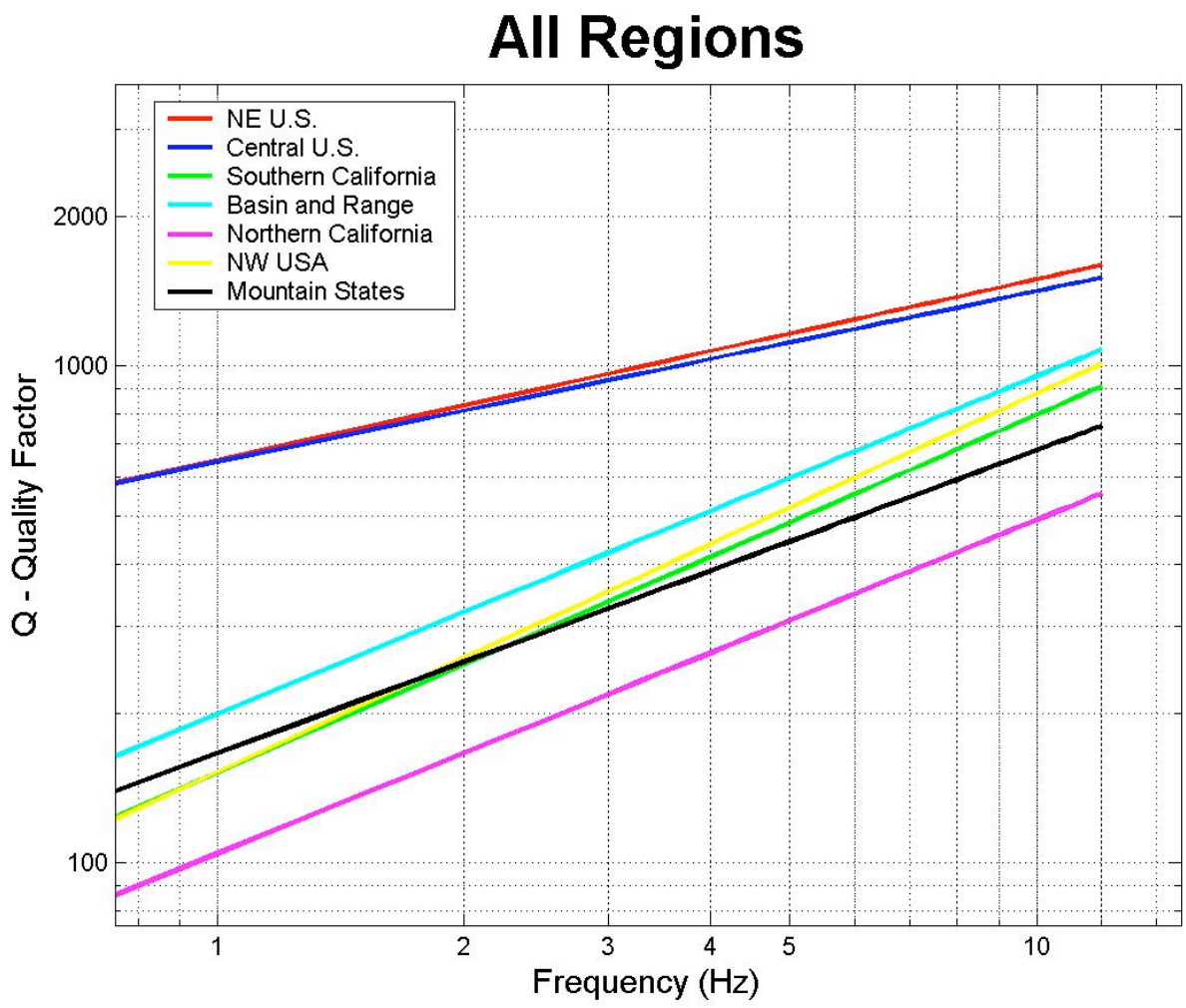
All Regions
NE U.S.
Central U.S.
Southern California
Basin and Range
Northern California
NW USA
Mountain States
2000
1000
100
Q - Quality Factor
1
2
3
4
5
10
Frequency (Hz)

Figure 10

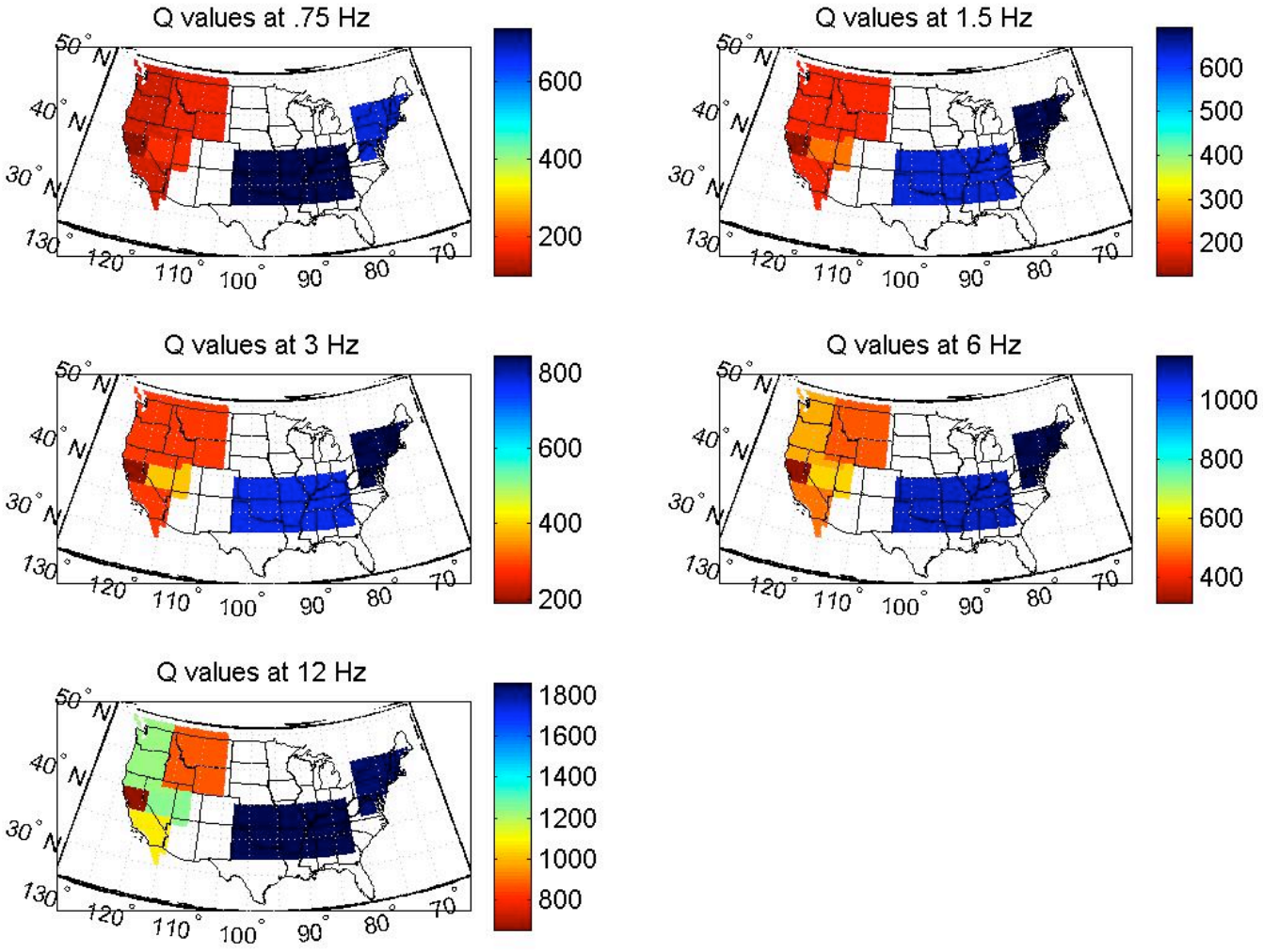
Q values at .75 Hz
600
400
200
Q values at 1.5 Hz
600
500
400
300
200
Q values at 3 Hz
800
600
400
200
Q values at 6 Hz
1000
800
600
400
Q values at 12 Hz
1800
1600
1400
1200
1000
800
50° N
40° N
30° N
130°
120°
110°
100°
90°
80°
70°

Figure 11